Editors: Cláudio T. Silva, csilva@cs.utah.edu
Daniel Weiskopf, weiskopf@visus.uni-stuttgart.de

GENERAL-RELATIVISTIC VISUALIZATION

By Thomas Müller and Daniel Weiskopf

General-relativistic visualization helps us understand what we could see when massive objects curve spacetime.

In our previous article about special-relativistic visualization,[1] we described what the travelers from our highly developed civilization observed when they passed the Earth; now, they set out for the Cygnus X-1 binary system, which is roughly 6,000 light years away. The Cygnus X-1 system consists of a super giant variable star (HDE 226868) and a very compact object—presumably a black hole—with about 11 times the mass of our Sun.[2] To make their journey as comfortable as possible, our travelers split their trip into two halves. In the first half, they accelerate with one Earth gravity (1 *g*), while in the second half, they decelerate again with 1 *g*. This simulates an artificial gravitation like on Earth.

Fortunately, our travelers can take advantage of the special-relativistic time dilation effect, which makes the trip last only 17 years with respect to their ship's chronometer. (Müller and his colleagues offer a detailed discussion of such a journey elsewhere.[3])

This time, the space ship captain will play it safe and order his crew to work out some tools in advance to simulate and explain any relativistic effects before they arrive at Cygnus X-1. The captain had heard rumors that a black hole devours all objects that come too close; in particular, the crew must find out how the curved spacetime around a black hole influences the propagation of light and the trajectories of massive objects. Again, we'll take up their challenge, asking how we can visualize general relativity's strange effects.

General Relativity

From special relativity, we already know that space and time are not two separate qualities, but rather are combined into a single entity: *spacetime*. While in special relativity spacetime is flat, general relativity uses curved spacetime to describe gravitational attraction geometrically. Although we have a certain notion about what a curved surface is in our everyday 3D world, we have extreme difficulties imagining how curvature "works" in a 4D non-Euclidean spacetime. Nonetheless, we can try to figure out what might be observed in curved spacetimes.

A most striking general-relativistic effect is the bending of light. Although a light ray locally always follows a straight line, its global trajectory is curved. The extent of the overall light deflection depends on the magnitude of the spacetime's curvature along the light ray's trajectory. In extreme situations, the curvature of some parts of the spacetime becomes so strong that even light cannot escape from that region. Hence, this region appears black and we call it a *black hole*. The region's separation surface is the *event horizon*. Figure 1 shows some examples of light rays around a black hole.

Today, the bending of light is important for astronomical observations because astronomers can use this effect as a *gravitational lens* to study objects that are so far away that they couldn't be observed otherwise. Figure 2 shows an example of gravitational lensing by the galaxy cluster Abell 2218, as recorded by the Hubble space telescope.

Figure 3 depicts a simplified situation to study general-relativistic effects on light caused by a black hole spacetime. Here, light from a distant star, *S*, reaches the observer via different paths and under different angles. Because the observer can trace back light rays only in a straight line, however, the star appears not at its actual position but as multiple images in the directions of the incoming light rays. If the star were directly behind the black hole, the observer would see an Einstein ring because of the spherical symmetry of the spacetime. Here, we depicted only two light rays between the star and the observer. In principle, there's an arbitrary number of light rays that orbit the black hole multiple times before they reach the observer, resulting in an equivalent number of apparent stars.

In addition to this geometric effect, the resulting phantom stars S_1 and S_2 also have different apparent luminosities compared to the star's actual luminosity: S_1 appears slightly brighter (7 percent), whereas S_2 has only one eighth of the original luminosity. That's because of the different (de)focusing and shearing effects of the curved spacetime on a bundle of light rays on the way between the star and the observer.

Additionally, the star's spectrum is altered. Depending on the relative

 1521-9615/11/$26.00 © 2011 IEEE

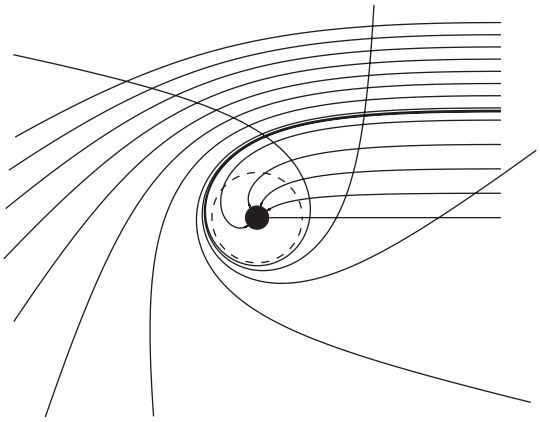

Figure 1. Light rays are bent due to curved spacetime; the bending becomes stronger the closer a light ray passes the black hole (black disk). Some light rays can also return to the point of emission. Hence, observers would see themselves as if in a strong distortion mirror. If a light ray passes the black hole too close (closer than the dashed circle), it will be captured and will move into the black hole.

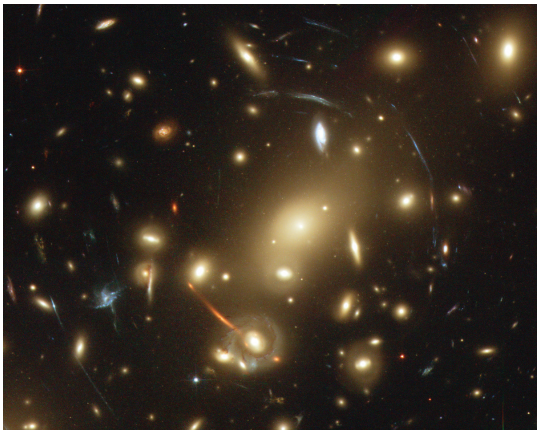

Figure 2. The galaxy cluster Abell 2218, composed of thousands of individual galaxies, works as gravitational lens for far distant galaxies that appear as long, thin arcs. This is a detail of the original picture by the Hubble space telescope (www.spacetelescope.org/images/heic0814a). — Image courtesy of NASA, European Space Agency (ESA), and Johan Richard, California Institute of Technology; with thanks to Davide de Martin and James Long (ESA/Hubble).

distances of the observer and the star to the black hole, light undergoes gravitational frequency shift. In this example, the star is a bit closer to the black hole than the observer, which results in a slight redshift of the star's spectrum. In short, a light ray gains energy when it's approaching the black hole and loses energy when it's receding from it. If the star's luminosity is time-dependent, we also must take into account the finite speed of light and the time dilation effect. In general, the different paths of the light rays have different spatial lengths, implying different light travel times. Furthermore, the closer a light ray passes the black hole, the slower time passes by. Thus, the star's luminosity variation will be observed at different times.

So far, we've considered only the motion of light. In case of the motion of massive objects in curved spacetime, we also must account for several other effects. For example, the geodesic precession and the Lense-Thirring effect are responsible for the change of an object's orientation when it orbits a black hole. The "Mathematical Details of General Relativity" sidebar offers a brief overview of the mathematical description of spacetimes, as well as the representation of light rays by lightlike geodesics and the trajectories of massive particles by timelike geodesics.

Diagram Techniques

We've already used a standard diagram technique to depict the paths of some light rays around a black hole in Figures 1 and 3. For that, we reinterpreted the intrinsic coordinates of the spacetime as the usual (pseudo) Cartesian coordinates and used the standard plotting software *gnuplot* (www.gnuplot.info). Generalizing this Cartesian-like illustration, we could also plot any doublet or triplet of the four coordinates in the diagram. It's important to note that, in the theory of relativity, time can also be a coordinate. In special relativity, the Minkowski diagram is an example of a diagram where time is plotted over one of the spatial coordinates, as we described in our previous article.[1]

The disadvantage of this technique is that it's explicitly coordinate-dependent while physics per se is coordinate-independent. For example, the coordinate distance between the observer and the black hole's horizon doesn't correspond to the actual distance. Hence, we must take care of the right interpretation of these diagrams. While standard plotting tools are sufficient for a first glimpse on how geodesics behave, a detailed geodesic exploration makes it necessary to interactively vary parameters, such as the initial position and direction of a geodesic or the intrinsic metric parameters.

The GeodesicViewer[4] provides a graphical user interface to realize this job. With an interactive tool, we can now investigate how light rays behave qualitatively in different regions of spacetime, thus understanding the structure of spacetime. In general relativity, we're also interested in a spacetime's causal structure and asymptotic properties. Hence, we need a method to compress the whole spacetime into a finite diagram while preserving its causal structure. Both Roger Penrose[5] and Brandon Carter[6] independently found such a transformation.

Figure 4 shows the 2D Penrose–Carter diagram of a Schwarzschild black hole. Here, the blue-shaded

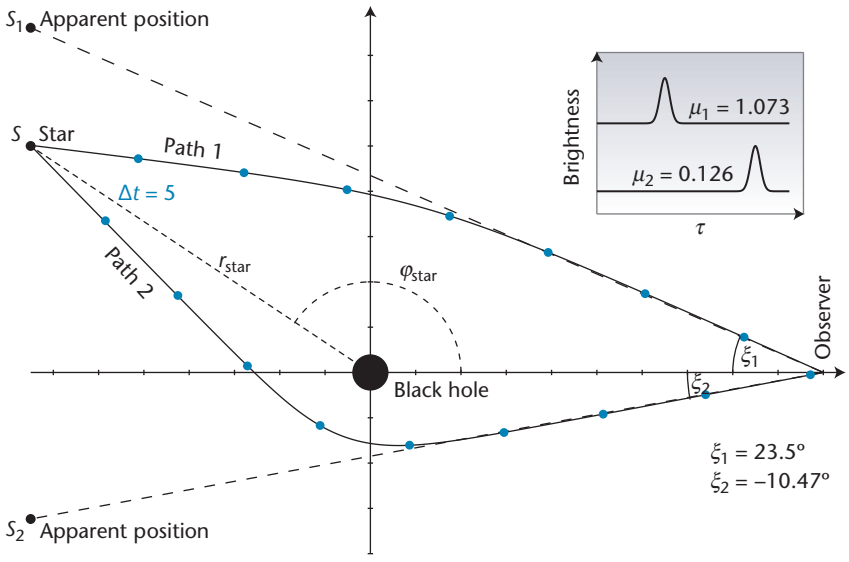

Figure 3. A simplified example of general-relativistic effects on light caused by a black hole spacetime. The main image shows apparent positions S_1 and S_2 of a star S located at (r_{star}, φ_{star}) whose light is deflected due to the curved spacetime in the neighborhood of a black hole. ξ_1 and ξ_2 are the incoming light directions with respect to the observer's local reference frame. The blue ticks ($\Delta t = 5$) indicate the elapsed time since the light emission. The inset (upper right) shows the temporal variation of the apparent brightness due to the gravitational lensing effect. The peaks correspond to a stellar eruption; there are different temporal delays for the different light paths.

region represents the inside and the square represents the "radial" outside of the black hole. The dashed line is the trajectory of a freely falling object that emits light rays (dotted lines) in the outward direction. As in the Minkowski diagram, light rays are lines with ± 45-degree slope.

The above techniques use coordinate mappings to show the influence of curved spacetime onto the trajectories of light rays or massive objects. Now, it would also be interesting to visualize the curvature of spacetime itself. However, because we have only an intuitive concept of 1D and 2D curvature in a 2D and 3D world, we're limited to a one- or 2D surface carved out from the full 4D spacetime. To visualize the curvature of this surface, we must find another surface embedded in the 3D Euclidean space that's *isometric* to the original surface—that is, distances on both surfaces

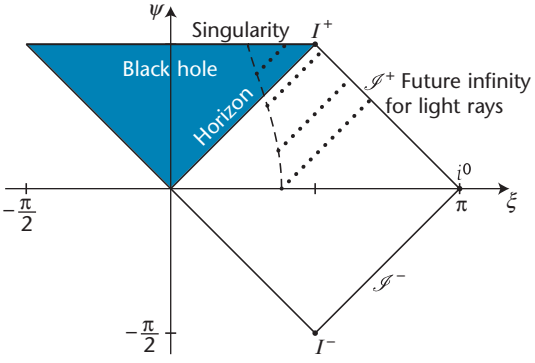

Figure 4. Penrose–Carter diagram of a Schwarzschild black hole. The dashed line represents an object that starts with zero velocity from outside the horizon and falls freely into the black hole. The dotted lines represent light rays emitted by this object. As long as the object is above the horizon, an observer outside the black hole can receive these light rays; the light rays eventually go infinitely far away from the black hole when time approaches infinity. This kind of infinity is drawn as line ($\mathscr{I}^+$). If the object is below the horizon, no single light ray can ever escape, and both the light rays and the object inevitably crash into the singularity. The boundary marks represent the so-called lightlike ($\mathscr{I}^+$), timelike ($I^\pm$), and spacelike (i^0) infinity, respectively. Also, while we show these boundary marks as points or lines, their true topology is much more complex.[7]

are preserved. In general, finding an embedding representation is by no means trivial, and is typically modeled by partial differential equations. A numerical method for solving the embedding problem might use a discretization with triangular meshes.[8,9]

Figure 5 shows a 2D surface cut out from a Schwarzschild black hole through its equatorial plane at constant time. The surface is isometrically embedded into the 3D Euclidean space. Here, the embedding is quite simple and can be represented by an ellipsoid of revolution because of the symmetry of the Schwarzschild spacetime and the location of the cutting plane on the equator.

First-Person Visualization

As in special relativity, first-person visualization in general relativity also aims to depict the image a virtual camera would actually produce in a general-relativistic setting. In contrast to the above diagram techniques, it has the additional advantage of being coordinate-independent. The generic approach for the first-person visualization is to extend the standard 3D ray tracing (see Figure 6) to relativistic ray tracing in 4D spacetime. (Weiskopf offers detailed technical background on general-relativistic ray tracing and further references on previous work elsewhere.[8])

For each pixel of the observer's virtual image plane, we must integrate the geodesic equation for light rays within the given spacetime instead of using just straight lines. We can stop the integration if one

Mathematical Details of General Relativity

Einstein's field equation, in today's form,

$$G_{\mu\nu} + \Lambda g_{\mu\nu} = \kappa T_{\mu\nu}$$

with $\kappa = 8\pi G/c^4$, Newton's gravitational constant G, the speed of light c, the cosmological constant Λ, and the metric $g_{\mu\nu}$, gives a relation between the geometry of spacetime, expressed by the Einstein tensor $G_{\mu\nu}$, and the stress-energy tensor $T_{\mu\nu}$, which represents mass density, and energy and momentum flux.

The most famous nontrivial solution to Einstein's field equation was found by Karl Schwarzschild in 1916. It describes the vacuum spacetime outside a static, spherically symmetric massive object—in particular, the outside of a black hole. The Schwarzschild metric, which defines infinitesimal distances, is given by the line element

$$ds^2 = -\left(1-\frac{r_s}{r}\right)c^2dt^2 + \frac{dr^2}{1-r_s/r} + r^2\left(d\vartheta^2 + \sin^2\vartheta d\varphi^2\right)$$

with the Schwarzschild radius $r_s = 2GM/c^2$ and the mass M of the object or black hole. The propagation of light as well as the trajectories of massive particles are determined by the geodesic equation

$$\frac{d^2x^\mu}{d\lambda^2} + \Gamma^\mu_{\nu\rho}\frac{dx^\nu}{d\lambda}\frac{dx^\rho}{d\lambda} = 0$$

with affine parameter λ and Christoffel symbols of the second kind $\Gamma^\mu_{\nu\rho}$, which are functions of the metric $g_{\mu\nu}$. The indices μ,ν,ρ run from 0 to 3. For the Schwarzschild spacetime, the coordinates read $x^\mu = \{t, r, \vartheta, \varphi\}$. The additional constraint,

$$g_{\mu\nu}\frac{dx^\mu}{d\lambda}\frac{dx^\nu}{d\lambda} = \kappa c^2$$

determines whether the geodesic describes massive particles ($\kappa = -1$, timelike geodesic) or light rays ($\kappa = 0$, lightlike geodesic). The gravitational frequency shift z_{grav} in the Schwarzschild spacetime,

$$1 + z_{\text{grav}} = \frac{\sqrt{1-r_s/r_{\text{obs}}}}{\sqrt{1-r_s/r_{\text{star}}}}$$

depends only on the relative distances r_{obs} and r_{star} to the black hole. A detailed introduction to general relativity can be found in the standard textbooks by Wolfgang Rindler[1] and Charles Misner, Kip Thorne, and John Wheeler.[2]

References

1. W. Rindler, *Relativity—Special, General, and Cosmological*, 2nd ed., Oxford Univ. Press, 2006.
2. C.W. Misner, K.S. Thorne, and J.A. Wheeler, *Gravitation*, W.H. Freeman and Co., 1973.

of the following conditions is met:

- the light ray hits an object,
- the light ray leaves the region of interest, or
- the numerical integration becomes invalid.

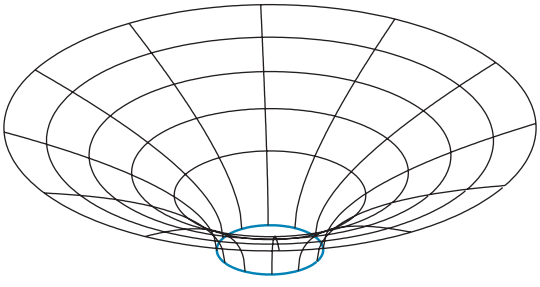

Figure 5. Isometric embedding of an equatorial plane through a Schwarzschild black hole. The blue circle represents the horizon. Only the surface is part of the Schwarzschild spacetime. Because of the Schwarzschild spacetime's staticity, a light ray or an object moving in the equatorial plane can be drawn onto the embedded surface.

Unfortunately, *shadow rays*, which connect directly to a light source, can be traced in practice only if there's an analytic solution of the geodesic equation. That's because it's nearly impossible to automatically find a ray between the intersection point and a light source in an arbitrarily curved spacetime. Additionally, there can be also more than just one connecting light ray.

Objects within general relativity can be defined either with respect to the metric's proper coordinates or with respect to a local reference (Minkowski) frame. The coordinate representation can be used, for example, to set a static global spherical background. The local reference description has the advantage that an object can be defined as static within the spatial part of the local frame, while the object's motion is assigned a property of the local frame. Then, the intersection of a light ray with a "local" object can be skipped if the light ray doesn't intersect with the boundary sphere of the local frame. The disadvantage, however, is that only objects that are small compared to the curvature's size can be used because the local reference frame is valid only for a small neighborhood.

What makes general-relativistic ray tracing so expensive is the calculation of the intersections between the curved light rays and the object's curved trajectories. In principle and without using special acceleration methods, every segment of the light ray must be tested against every trajectory segment of each single object. Because light rays don't interact, 4D ray tracing can be easily

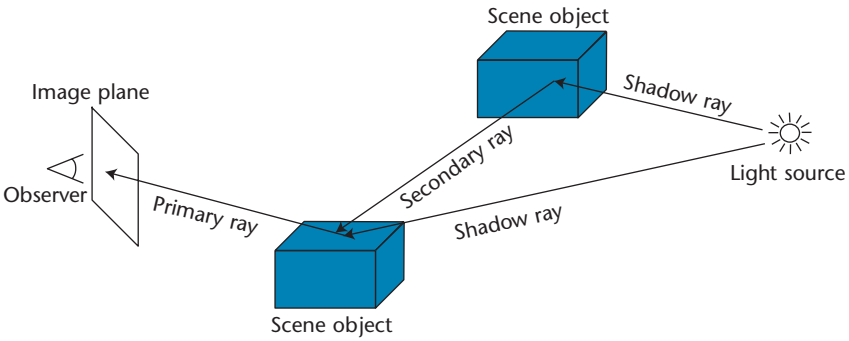

Figure 6. For each pixel of the observer's virtual image plane, standard 3D ray tracing follows a rectilinear light ray into the scenery. Depending on the illumination model, for each intersection point one or more secondary rays are tracked and shadow rays to the light sources are determined.

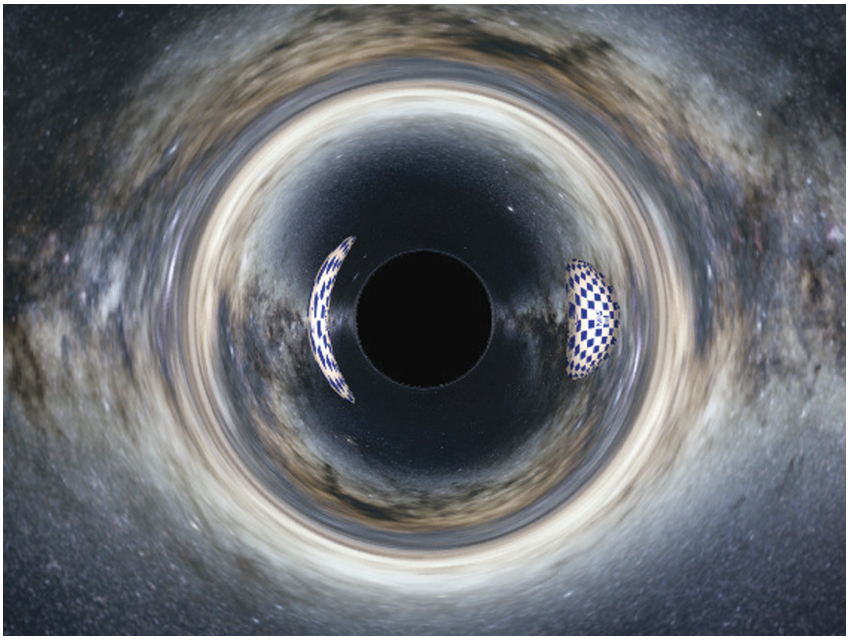

Figure 7. A star textured with a spherical grid passes behind a black hole. Due to light bending, the star appears not only distorted but also twice, where the secondary image (left) is mirrored. The Milky Way panorama is also distorted by the curved light rays. The image is produced using the CUDA-based general relativistic ray tracer by Daniel Kuchelmeister.[10] The slight shading on the star was artificially added to enhance the 3D impression. — The Milky Way panorama is by Serge Brunier, European Southern Observatory.

parallelized by image-space partitioning, for example, on a compute cluster or using modern graphics hardware and the Compute Unified Device Architecture (CUDA; http://developer.nvidia.com/cuda) or the Open Computing Language (OpenCL; www.khronos.org/opencl) programming interface.

Figure 7 shows the first-person view of a star that passes behind a black hole. The star is a sphere with a diameter three times the Schwarzschild radius defined within a local reference frame that currently moves at 90 percent the speed of light. Because of the bending of light, the star appears distorted and on both sides of the black hole. The background is a coordinate sphere textured with the Milky Way panorama. Here, we applied only the geometric distortion effects. For the gravitational redshift and the lensing effect, we would need complete spectral information of the Milky Way panorama.

The main problem of general-relativistic visualization is the search for geodesics that connect two arbitrary points in spacetime. If a spacetime is highly symmetric and there's an analytic solution to the geodesic equation, an interactive visualization becomes feasible, because we're now able to find light rays that connect two points in spacetime. Connecting light rays is key to rendering algorithms that project objects of the scene onto the image plane. Just like regular 3D nonrelativistic graphics, we can now efficiently process scene object after scene object and determine their image on the viewing plane by rasterizing their image footprint into corresponding pixels.

Figure 8 shows an example of projection and rasterization: we use the analytic solution[11] to the geodesic equation in the Schwarzschild spacetime to simulate the distortion of the stellar sky by a black hole.[12] Because of the spherical symmetry of the Schwarzschild spacetime, the search for an interconnecting light ray between a star and the observer can be restricted to the 2D situation analogous to Figure 1. Here, we assume that all stars have distances to the black hole that are much larger than the observer's distance to the black hole so that we can put the stars at infinity to reduce the positional information to a single angle. Then, in a preprocessing step, we can generate a 2D lookup table that stores for each observer position $r_{obs} \in [r_s, r_{max}]$ and each star position $\varphi_{star} \in [0, 2\pi)$ the corresponding angular directions ξ_1 and ξ_2 for the primary and secondary apparent directions. (Here, we could also store higher-order apparent directions. But, because of the gravitational lensing effect, the apparent

luminosity of higher-order images strongly decreases.)

For this example of the stellar sky's distortion by a black hole, we illustrate how point-based visualization can be efficiently implemented on graphics hardware. We assume that the reader is familiar with the terminology from GPUs as briefly reviewed in our previous article on special-relativistic visualization.[1] As input for the algorithm, we store the 2D lookup table in a 2D texture. Each star is assigned a 2D vertex (point) with spherical coordinates (right ascension and declination) and two additional attributes: its apparent magnitude (observed scaled flux density) and effective color temperature.

In the first render pass, the vertex program calculates the effective angle φ_{star} of a star from its right ascension and declination and, by means of the lookup table, determines the apparent angle ξ with respect to the observer's local reference frame. (The apparent star is located on the plane spanned by the direction to the black hole and the direction to the star.) The star's apparent magnitude, which is modified by the gravitational lensing effect and the observer's current velocity, is mapped to the size of the vertex. The frequency shift due to the observer's motion and gravitation determines the star's apparent color temperature. After the rasterizer, the fragment program maps the color temperature to a predefined color table and smears the point to a Fraunhofer diffraction pattern caused by the finite aperture of a telescope. In the second render pass, the higher-order images of the stars are drawn.

The points-based visualization technique can also be applied to expanded objects defined in a local reference frame in highly complex spacetimes, such as the Gödel universe as done by Frank Grave and his colleagues.[13]

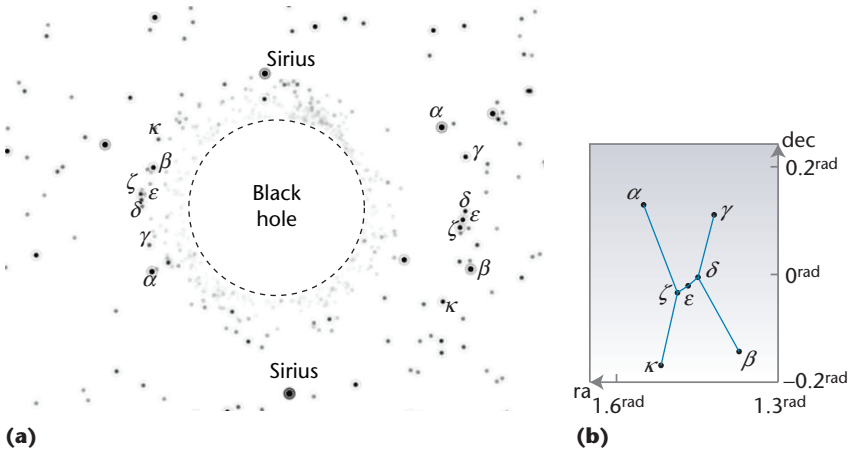

Figure 8. Projection and rasterization. (a) Constellation Orion distorted by the curved spacetime of a black hole indicated by the dashed circle. Stars appear twice because of light rays that pass the black hole to the left and to the right. The rings around the stars simulate the Fraunhofer diffraction due to the finite telescope aperture. The star database is taken from the Hipparcos catalogue (I/239), which can be found at http://cdsarc.u-strasbg.fr/viz-bin/Cat?I/239. (b) Constellation Orion (α: Betelgeuse, β: Rigel, γ: Bellatrix, δ: Mintaka, ε: Alnilam, ζ: Alnitak, κ: Saiph) given in undistorted equatorial coordinates (ra: right ascension, dec: declination).

Field-Based Data Visualization

The techniques we've described are usually applied to spacetimes that can be described mathematically in closed form. However, realistic astrophysical scenarios of interest—such as the merger of two rotating black holes—can be handled only by extensive numerical simulation.

Thomas Baumgarte and Stuart Shapiro provide a detailed introduction to numerical relativity.[14] Much research in numerical relativity deals with possible shapes of gravitational waves induced by, for example, collapsing stars, oscillating neutron stars, or black hole mergers. For that, the numerical calculations often use grid-based techniques. In particular, adaptive mesh refinement techniques, known also from computational fluid dynamics, are heavily used to meet the concerns of the very different strengths of curvature in the respective domains. In general, scientific visualization supports the visual analysis and communication of grid-based data from the physical sciences. Therefore, classical scientific visualization techniques—such as color-coding techniques, isosurface rendering, volume visualization, and glyph representations—work for simulation data from general relativity.

In the *Visualization Handbook*, Charles Hansen and Chris Johnson provide a comprehensive overview of scientific visualization's methods, software systems, and applications.[15] One issue specific to general relativity is that the visualization results shown should be physically relevant. Here, the dependency of numerical data on the chosen coordinate system or reference frame plays an important role. Because general relativity is usually described in the tensor formalism, relevant information is commonly extracted in the form of tensor fields or in derived vector or scalar fields. This kind of field data is then handed over to the visualization system.

As an example, Figure 9 shows isosurfaces of the Newman-Penrose curvature scalar Ψ_4 for a simulation of gravitational waves produced by the merger of two black holes. For examples of tensor visualization, we refer to the work of Werner Benger and Hans-Christian Hege,[16] who discuss

the direct visualization of the metric tensor for the static Schwarzschild or the rotating Kerr spacetime using tensor ellipsoids and tensor splats.

Due to general relativity's complexity, there's a wide range of visualization techniques, each specializing in certain facets of curved spacetime. Diagrams for general relativity are often manually drawn with generic graphics software or generated by basic plotting tools; they're used for visual explanation in textbooks or other examples of the didactics of physics. Advanced diagram techniques—such as the Penrose–Carter diagram—are used by relativity experts to visualize a spacetime's causal structure.

In contrast to the abstraction of diagrams, the general-relativistic first-person visualization provides a more immersive view. We, as beholder, take part in a visual experiment by being included as direct observer of the physical scenario. Such visual experiment is conceptually simple and therefore especially useful in the context of teaching, visual communication to non-experts, museum exhibitions, and so on. First-person visualization comes with high computational costs for rendering scenes in 4D spacetime, such as in applying general-relativistic ray tracing or projection methods.

Finally, for simulation data from numerical relativity, it's possible to use standard methods and software systems for scientific visualization, as long as the data is provided in processable form, such as a tensor, vector, or scalar field.

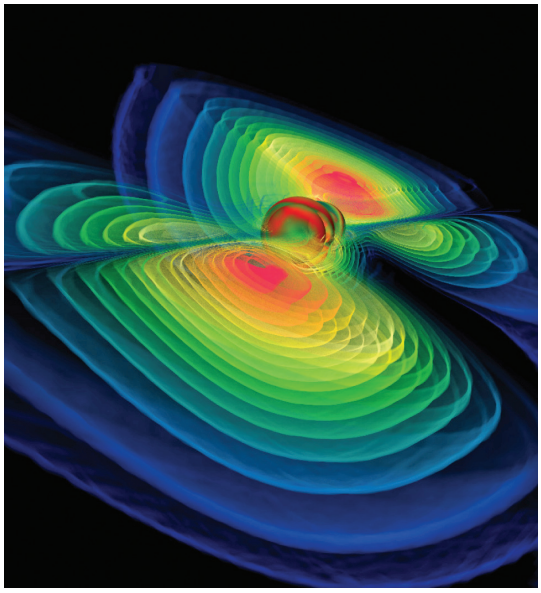

Figure 9. An image based on simulations of the gravitational waves produced by the merger of two black holes in full numerical relativity.[17] The black holes are represented by colored "balls" (actually the so-called apparent horizons), where the color indicates the local Gauss curvature. The wavy features are iso-surfaces based on the Newman-Penrose scalar Ψ_4, which is an indicator for the emitted gravitational energy. — Image courtesy of Werner Benger (MPI for Gravitational Physics, Zuse Institute Berlin, Center for Computation & Technology at Louisiana State University), 2001.

Acknowledgments

This work was partially funded by Deutsche Forschungsgemeinschaft (DFG) as part of the Collaborative Research Centre SFB 716 and the DFG Astrographik project.

References

1. T. Müller and D. Weiskopf, "Special-Relativistic Visualization," *Computing in Science & Eng.*, vol. 13, no. 4, 2011, pp. 85–93.
2. S.M. Caballero-Nieves et al., "The Ultraviolet Spectrum and Physical Properties of the Mass Donor Star in HD 226868=Cygnus X-1," *The Astrophysical J.*, vol. 701, no. 2, 2009, pp. 1895–1905.
3. T. Müller, A. King, and D. Adis, "A Trip to the End of the Universe and the Twin 'Paradox,'" *Am. J. Physics*, vol. 76, no. 4, 2008, pp. 360–373.
4. T. Müller and F. Grave, "Geodesic-Viewer—A Tool for Exploring Geodesics in the Theory of Relativity," *Computer Physics Comm.*, vol. 181, no. 2, 2010, pp. 413– 419.
5. R. Penrose, "Zero Rest-Mass Fields Including Gravitation: Asymptotic Behaviour," *Proc. Royal Society London*, series A, Mathematical and Physical Sciences, vol. 284, no. 1397, 1965, pp. 159–203.
6. B. Carter, "Complete Analytic Extension of the Symmetry Axis of Kerr's Solution of Einstein's Equations," *Physical Rev.*, vol. 141, no. 4, 1966, pp. 1242–1247.
7. C.W. Misner, K.S. Thorne, and J.A. Wheeler, *Gravitation*, W.H. Freeman and Co., 1973.
8. D. Weiskopf, *Visualization of Four-Dimensional Spacetimes*, PhD thesis, Univ. Tübingen, 2001; http://tobias-lib.uni-tuebingen.de/volltexte/2001/240.
9. M. Isenburg, S. Gumhold, and C. Gotsman, "Connectivity Shapes," *Proc. IEEE Visualization Conf.*, IEEE CS Press, 2001, pp. 135–142.
10. D. Kuchelmeister et al., "CUDA-Based General Relativistic Ray Tracer," forthcoming, 2012.
11. S. Chandrasekhar, *The Mathematical Theory of Black Holes*, Oxford Univ. Press, 1983.
12. T. Müller and D. Weiskopf, "Distortion of the Stellar Sky by a Schwarzschild Black Hole," *Am. J. Physics*, vol. 78, no. 2, 2010, pp. 204–214.
13. F. Grave et al., "The Gödel Engine—An Interactive Approach to Visualization in General Relativity," *Computer Graphics Forum*, vol. 28, no. 3, 2009, pp. 807–814.
14. T.W. Baumgarte and S.L. Shaprio, "*Numerical Relativity: Solving Einstein's Equations on the Computer*, Cambridge Univ. Press, 2010.
15. C.D. Hansen and C.R. Johnson, eds., *The Visualization Handbook*, Elsevier, 2005.

Web Resources

Following are lists of resources that we've found particularly relevant.

General-Relativistic Visualization

The Web offers several useful resources for general-relativistic visualization:

- Field-based data visualizations for general relativistic situations, such as binary systems or gravitational collapses, are provided by the Numerical Relativity Group (http://numrel.aei.mpg.de) at the Albert Einstein Institute in Golm, Germany.
- The Visualization in Special and General Relativity website (www.vis.uni-stuttgart.de/relativity), which we maintain at the University of Stuttgart, Germany, provides several interactive applications, including the GeodesicViewer for detailed explorations of lightlike and timelike geodesics.
- Space Time Travel (www.spacetimetravel.org), maintained by Ute Kraus and Corvin Zahn at the University of Hildesheim, Germany, includes many images and videos of black hole and wormhole visualizations. In particular, this site features many didactics papers that explain special relativity.
- Robert Nemiroff, Michigan Technological University and NASA Goddard, offers movies that show the visual distortion effects near a black hole and neutron stars (http://apod.nasa.gov/htmltest/rjn_bht.html) and also provides an accompanying paper.[1]
- Andrew Hamilton, University of Colorado at Boulder, provides movies that show the inside of a black hole (http://jila.colorado.edu/~ajsh/insidebh/index.html).
- Leo Brewin, Monash University, Australia, offers relativity movies (http://users.monash.edu.au/~leo/research/movies/index.html).

Astrophysics Resources

Additional resources on astrophysics are available on the following Web pages:

- The Hubble Space Telescope Web page by ESA (www.spacetelescope.org) includes pictures and illustrative movies of gravitational lensing in action.
- NASA offers an illustration of the Cygnus X-1 system (http://apod.nasa.gov/apod/ap080811.html).
- More detailed information on the binary system Cygnus X-1 is available in many places, including in the paper by Saida Caballero-Nieves and her colleagues.[2]

References

1. R.J. Nemiroff, "Visual Distortions Near a Neutron Star and Black Hole," *Am. J. Physics*, vol. 61, no. 7, 1993, pp. 619–632.
2. S.M. Caballero-Nieves et al., "The Ultraviolet Spectrum and Physical Properties of the Mass Donor Star in HD 226868=Cygnus X-1," *The Astrophysical J.*, vol. 701, no. 2, 2009, pp. 1895–1905.

16. W. Benger and H.-C. Hege, "Analysing Curved Spacetimes With Tensor Splats," *The 10th Marcel Grossmann Meeting—Recent Developments in Theoretical and Experimental General Relativity, Gravitation and Relativistic Field Theories*, M. Novello, S. Perez-Bergliaffa, and R. Ruffini, eds., World Scientific, 2006, pp. 1619–1626.
17. M. Alcubierre et al., "3D Grazing Collision of Two Black Holes," *Physical Rev. Letters*, vol. 87, no. 27, 2001, pp. 271103-1—4.

Thomas Müller is a post-doctoral researcher at the University of Stuttgart, Germany. His research interests include visualization, GPU methods, and special and general relativity. Müller has a PhD (Dr. rer. nat.) in physics from the University of Tübingen, Germany. He is a member of the German Physical Society. Contact him at Thomas.Mueller@visus.uni-stuttgart.de.

Daniel Weiskopf is a professor at the University of Stuttgart, Germany. His research interests include visualization, visual analytics, GPU methods, computer graphics, and special and general relativity. Weiskopf has a PhD (Dr. rer. nat.) in physics from the University of Tübingen, Germany. He is a member of IEEE Computer Society, ACM Siggraph, and the German Society for Computer Science (Gesellschaft für Informatik). Contact him at weiskopf@visus.uni-stuttgart.de.